Journal of ELECTRONIC MATERIALS, Vol. 43, No. 11, 2014
DOI: 10.1007/s11664-014-3363-3

Investigating the Exchange-Coupling Interaction in Nanostructure Composite Particles of $SrFe_{12}O_{19}$ and $ZnFe_2O_4$

M. MEHDIPOUR,[1,3] H. SHOKROLLAHI,[2] and A. BAHADORAN[1]

1.—Department of Materials Engineering, Faculty of Mechanical Engineering, University of Tabriz, 5166-16471 Tabriz, Iran. 2.—Electroceramics Group, Materials Science and Engineering Department, Shiraz University of Technology, 71555-313 Shiraz, Iran. 3.—e-mail: mostafa_mehdipour67@yahoo.com

Ferromagnetic $SrFe_{12}O_{19}$–$ZnFe_2O_4$ nanostructure composite particles were synthesized by co-precipitation of chloride salts, in different stoichiometric ratios, by addition of sodium hydroxide solution. The resulting precursors were heat treated at temperatures in the range 800–1200°C for 4 h. Exchange interactions of the nanostructure composite particles were studied by use of exchange-coupling theory and plots of magnetic hysteresis. On the basis of exchange-coupling theory, the exchange interaction can be improved by increasing the soft phase content within the hard matrix. As temperature and soft phase ratio increase, the exchange interaction increases because of exchange length enhancement. The modified Brown's equation was also used to analyze the effects of exchange coupling on coercivity.

Key words: Nanostructure composite particles, co-precipitation, exchange coupling, modified Brown's equation

INTRODUCTION

Exchange-coupled nano-composite magnets, which are good candidates for advanced permanent magnetic applications because of their large energy production,[1] contain magnetically hard and soft phases that interact by magnetic exchange coupling.

Exchange coupling is a preference for specific relative orientations of the moments of two different magnetic materials when they are in intimate contact with each other or are separated by a sufficiently small distance (≤60 Å). This enables spin information to be communicated between the two materials. One material is, usually, magnetically soft and the other magnetically hard (or antiferromagnetic). Exchange coupling is manifested as a displacement of the hysteresis loop of the soft material along its field axis.[2] Exchange coupling occurs over the exchange length $l_{ex} = (A/K)^{.5}$, where A is the exchange stiffness and K the magneto crystalline anisotropy constant. For nanocomposites, A and K can be described as the effective exchange stiffness and effective anisotropy constant, respectively.[3]

In the co-precipitation method, precipitation is achieved by adding a mixed solution of chloride cations (Fe, Sr and Zn) dropwise to NaOH or Na_2CO_3 solution.[4–7] Carbonates or nitrates can be used in place of chlorides to synthesize hexaferrites.[8,9] Heat treatment makes the process fast, and hexaferrite particles crystallize completely as hexagonal pyramidal or plate-like shapes after cooling in the furnace.[10,11] Similar morphology was obtained by Tyagi et al. for $SrFe_{11.2}Zn_{.8}O_{19}$[12] and $SrFe_{11}Ni_{.5}Zn_{.5}O_{19}$.[13]

In this investigation nanostructure composite particles of $SrFe_{12}O_{19}$ and $ZnFe_2O_4$ were synthesized by co-precipitation, and the effects of stoichiometric ratio and subsequent treatment temperature were studied. Compared with other methods this is a low-cost technique suitable for mass production.[12,14–16] Single-phase-like smooth variation of magnetization with applied field was

(Received May 8, 2013; accepted August 1, 2014; published online September 5, 2014)

observed, indicating that the nanostructure composite particles are effectively exchange coupled and that magnetization of the hard and soft phases reverses cooperatively. The modified Brown's equation was used to analyze the effect of exchange coupling on coercivity.

EXPERIMENTAL

In this investigation, analytical-grade ferric chloride ($FeCl_3$, $6H_2O$), strontium chloride ($SrCl_2$, $6H_2O$), zinc chloride ($ZnCl_2$), and NaOH were used to synthesize the ($SrFe_{12}O_{19}$–$ZnFe_2O_4$) nanostructure composite particles by co-precipitation. Appropriate stoichiometric amounts of strontium, ferric, and zinc chlorides were completely dissolved in ultrapure water and brownish-colored ferrite particles were precipitated from the mixtures by gradual addition of sodium hydroxide (NaOH) solution (pH 12) at room temperature. The aqueous suspension was stirred gently for 15 min to achieve good homogeneity. The precipitates were then isolated by filtration, washed with water, and dried at 100°C overnight. The as-synthesized particles were heated at 10°/min to temperatures in the range 800–1200°C then maintained at that temperature for 4 h.

Phase identification of the annealed samples was performed by x-ray diffraction (XRD; Siemens, D5000 diffractometer with Cu K_x radiation). Average crystallite size of the powder was determined by use of Scherer's formula. Reaction kinetics for formation of the nanostructure composite particles were studied by differential thermal analysis (DTA) and thermogravimetry (Shimadzu DTG-66AH). Morphology was studied by scanning electron microscopy (SEM; Hitachi S4160 and Vega TEscan). Magnetic measurements were performed at room temperature in the applied field range −10 kOe to 10 kOe by use of a magnetometer (Magnet-Physik C-300).

RESULTS AND DISCUSSION

The indexed XRD patterns of the $SrFe_{12}O_{19}$–$ZnFe_2O_4$ nanostructure composite particles in the as-synthesized state and after treatment at temperatures from 800–1200°C for 4 h (I), and for different stoichiometric ratios (II), are shown in Fig. 1. From the results, it can be inferred that the hexaferrite powder in the as-synthesized condition contains NaCl only as impurity (JCPDS card no. 5-637). When annealed at 1200°C, $SrFe_{12}O_{19}$ ($2\theta = 34.198^\circ$, d = 2.61983 Å; JCPDS card no. 01-072-0739) and $ZnFe_2O_4$ ($2\theta = 35.452^\circ$, d = 2.53000 Å; JCPDS card no. 00-001-1109) were synthesized. This indicates that in the as-synthesized condition the structure is a mixture of amorphous nanostructure composite particles of $SrFe_{12}O_{19}$ and $ZnFe_2O_4$, and that calcination is needed for crystallization. As expected, the crystallinity and the amount of soft phase increased when the heat-treatment temperature (HT) was increased from 800°C to 1200°C and when the Zn-to-Sr stoichiometric ratio was increased. The intensity of the maximum peak of the $SrFe_{12}O_{19}$ phase (as a measure of the amounts of the phases) was found to increase when HT was increased—from 44.89 cts at 800°C to 52.18 cts at 1200°C. Other information about the extent of phase change is listed in Tables I and II.

SEM micrographs of the ferrite powder as-synthesized and after heat treatment at temperatures from 800°C and 1200°C are shown in Fig. 3. In the as-synthesized condition the particles seem to have spherical morphology with particle size in the range 20–25 nm (Fig. 2a). With increasing HT, the particles grow and different morphology is observed (Fig. 2b and c).

SEM micrographs of ferrite powder of different stoichiometric ratio after heat treatment at 1100°C are shown in Fig. 3. The particles of the single hard $SrFe_{12}O_{19}$ phase seem to have hexagonal morphology with an average particle size of approximately 5 μm (Fig. 3a). When the stoichiometric ratio is increased different morphology is observed (Fig. 3b and c). This can be attributed to the effect on the kinetics, in accordance with the Johnson–Mehl–Avrami (JMA) equation.[17]

To study the microstructure of the composite particles, back-scatter electron (BE) images of composite particles of different stoichiometric ratio treated at 1100°C were acquired; these are shown in Fig. 4. It is clear that a separation phase is observed for the composite state but not for the single phases. The parts shown in black can be related to $SrFe_{12}O_{19}$, because these parts decrease on increasing the Zn/Sr ratio. The EDX spectra of the soft and hard phases (for the composite with Zn/Sr = 1) confirm these changes. These results from the BE images again prove composite particles have been synthesized, and confirm the XRD results.

Magnetic measurements of the $SrFe_{12}O_{19}$–$ZnFe_2O_4$ nanostructure composite particles showed coercivity and remanence were almost negligible in the as-synthesized condition (Fig. 4), indicative of the paramagnetic behavior of the material. However, when the as-synthesized powders were heat treated at 800°C to 1200°C, the particles were transformed from paramagnetic to ferromagnetic. Their saturation magnetization (J_s) was found to depend on the HT, increasing from 0 kG to 0.85 kG with increasing temperature (Fig. 4). The increase in the saturation magnetization can be explained as follows:

1. crystalline magnetic phase formation: formation of strontium hexaferrites and zinc ferrite, as confirmed by the x-ray study of the powder heat treated at 1200°C (Fig. 1); and
2. particle size: as average particle size increases, magnetic ordering increases[18] (Table I).

As the heat-treatment temperature is increased from 800 to 1200°C, the magnetic coercivity decreases from 5.6 kOe to 0.09 kOe (Fig. 4). This is

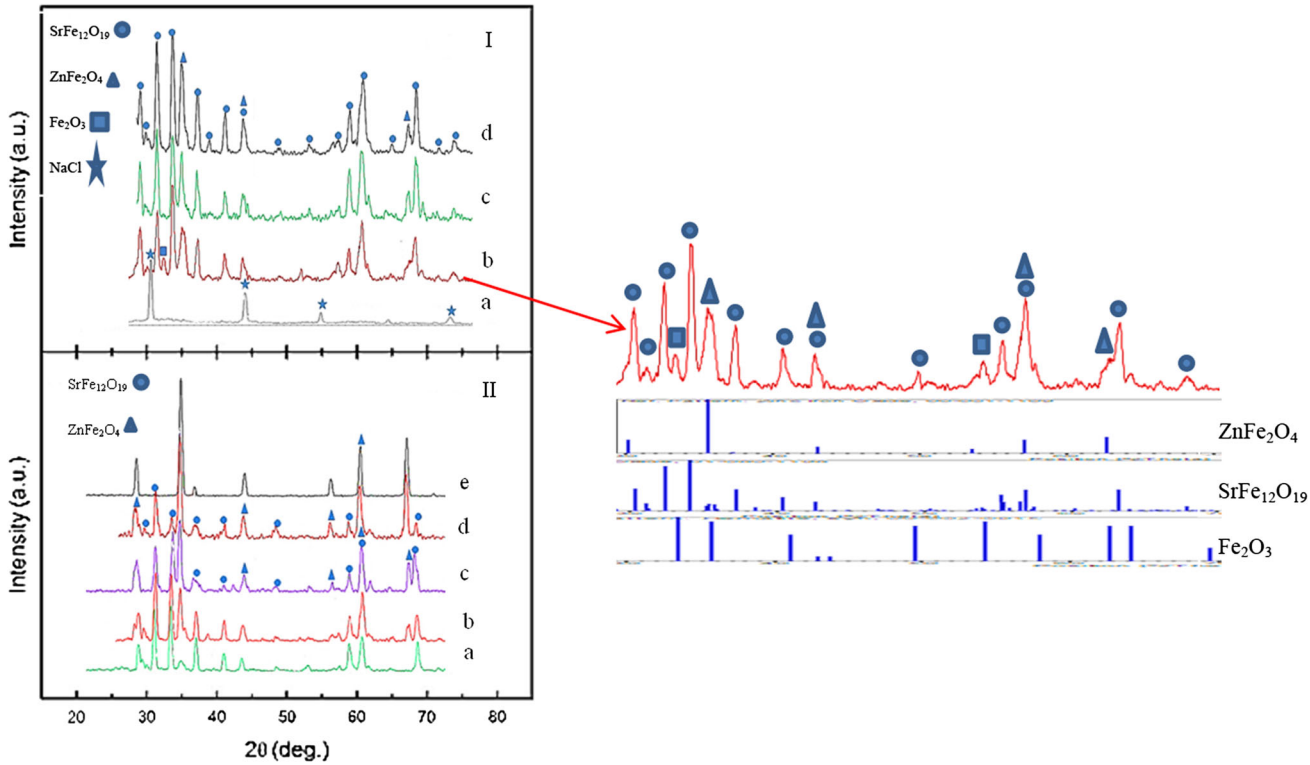

Fig. 1. (I) XRD patterns of the $SrFe_{12}O_{19}$–$ZnFe_2O_4$ nanostructure in the as-synthesized state (I-a) and after heat treatment at 800°C (I-b), 1000°C (I-c), and 1200°C(I-d). (II) XRD patterns of the $SrFe_{12}O_{19}$–$ZnFe_2O_4$ nanostructure with different stoichiometric ratios after heat treatment at 1100°C: (II-a) $SrFe_{12}O_{19}$ (II-b) Zn/Sr = 1 (II-c) Zn/Sr = 2 (II-d) Zn/Sr = 3 (II-e) $ZnFe_2O_4$.

Table I. Effect of temperature on the intensity of the maximum peaks of $SrFe_{12}O_{19}$ and $ZnFe_2O_4$

	800°C	1000°C	1200°C
Intensity of the maximum peak of $SrFe_{12}O_{19}$	44.89 cts	50.12 cts	52.18 cts
Error bar	33.45	34.56	33.19
Intensity of the maximum peak of $ZnFe_2O_4$	24.74 cts	35.54 cts	37.23 cts
Error bar	32.92	33.84	31.65

Table II. Effect of stoichiometric ratio on the intensity of the maximum peaks of $SrFe_{12}O_{19}$ and $ZnFe_2O_4$

	Sr	Zn/Sr = 1	Zn/Sr = 2	Zn/Sr = 3	Zn
Intensity of the maximum peak of $SrFe_{12}O_{19}$	50.13 cts	49.24 cts	47.17 cts	40.14 cts	0 cts
Error bar	30.15	31.76	31.36	33.57	32.21
Intensity of the maximum peak of $ZnFe_2O_4$	0 cts	23.16 cts	50.09 cts	70.19 cts	78.44 cts
Error bar	35.35	31.52	32.71	30.55	33.24

because of an increase in the exchange-coupling interaction[19] and can be explained as follows. Theoretical studies suggest that for hard and soft phases to reverse cooperatively in the hard–soft composite system, the critical dimension of the soft phase (t_s) should be less than twice the domain wall width (δ_w) of the hard phase.[2] However, the critical dimension of the soft phase (t_s) should depend on the ratio of the soft phase to the hard phase.[20] The crystallite size of the soft phase for different

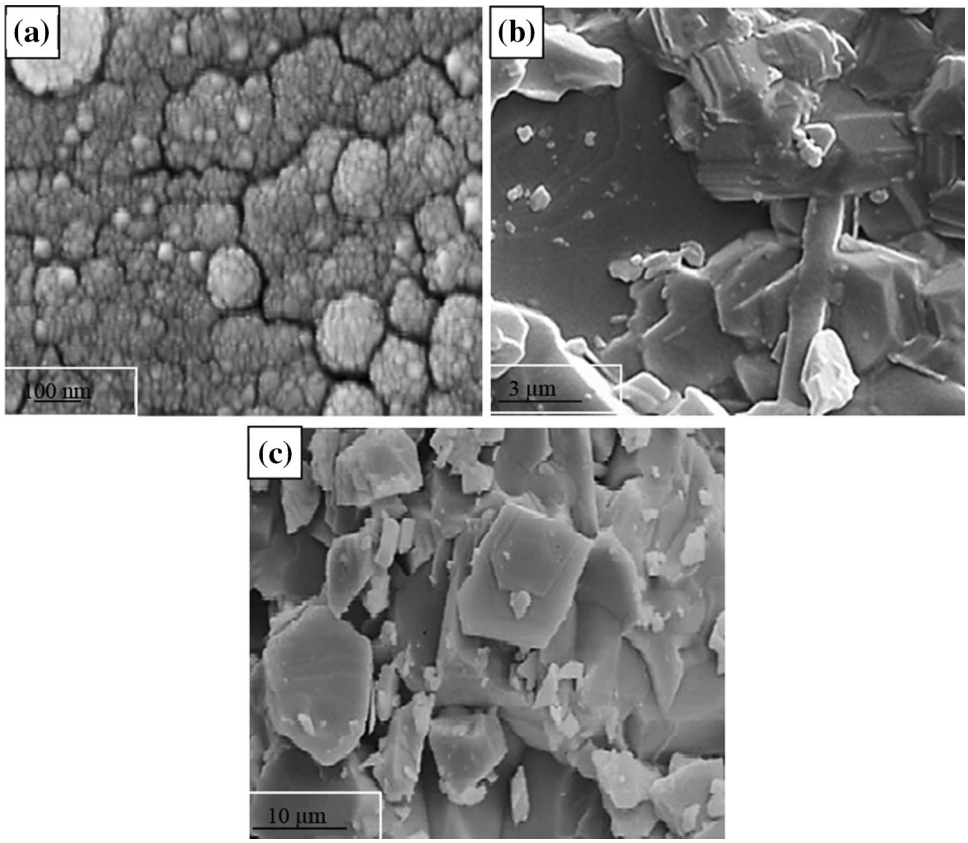

Fig. 2. SEM micrographs of ferrite powder as-synthesized (a) and after heat treatment at 800°C (b) and 1200°C (c).

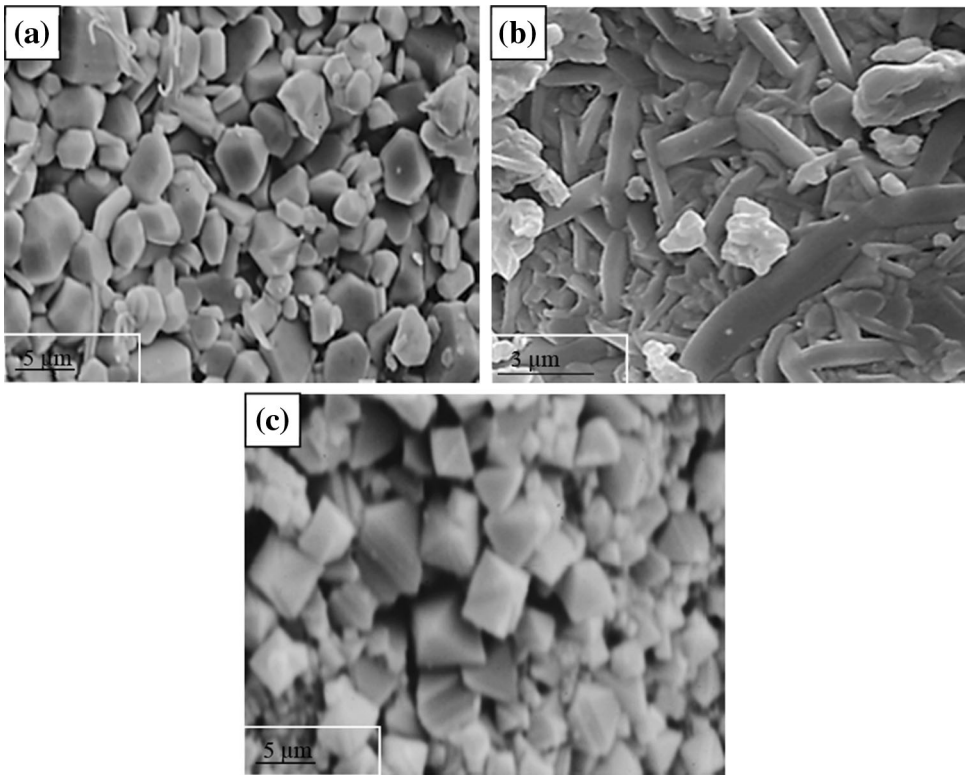

Fig. 3. SEM micrographs of ferrite powder of different stoichiometric ratio heat treated at 1100°C: (a) $SrFe_{12}O_{19}$ (b) Zn/Sr = 2 (c) $ZnFe_2O_4$.

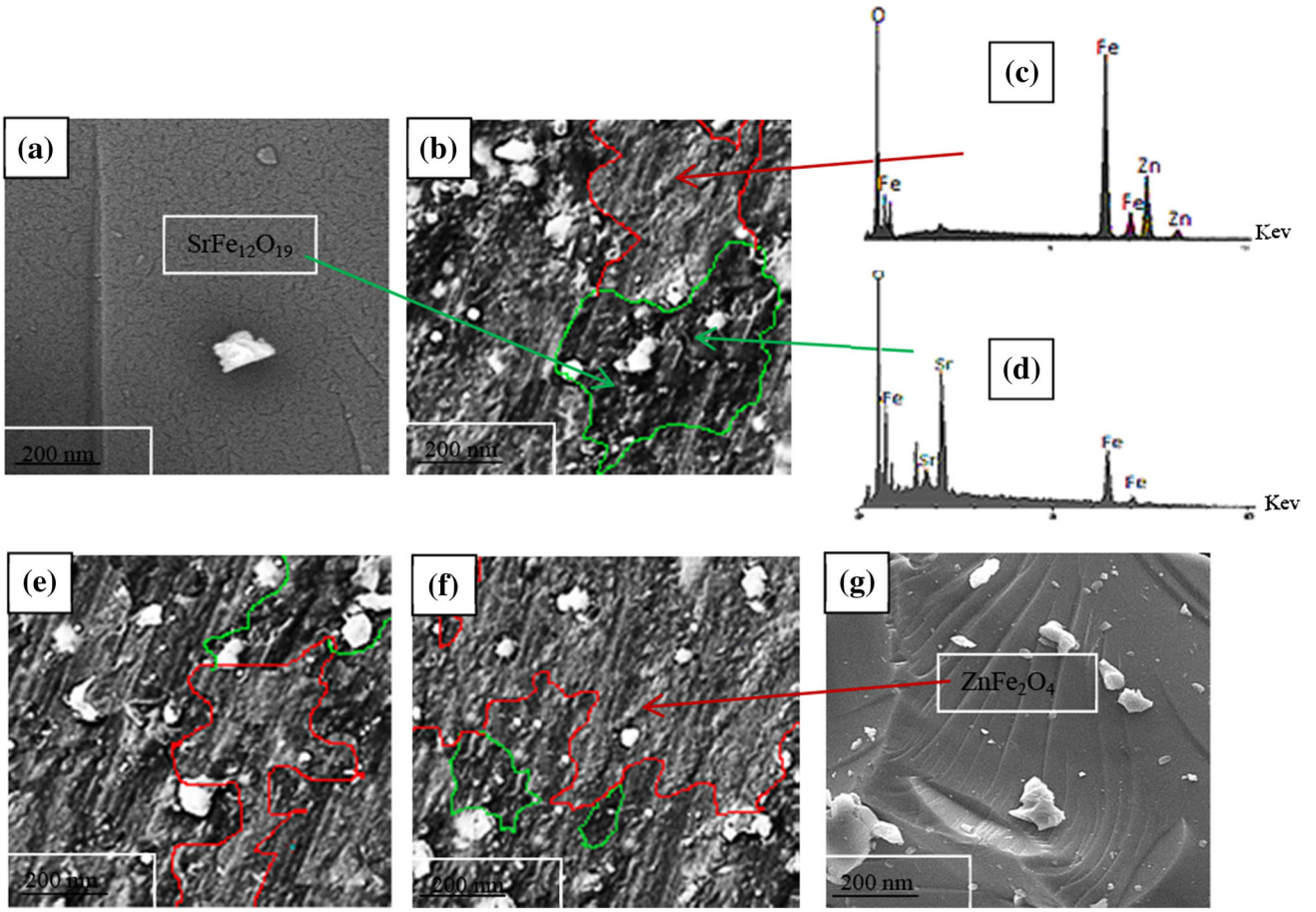

Fig. 4. BE images of ferrite particles of different stoichiometric ratio treated at 1100°C: (a) $SrFe_{12}O_{19}$; (b) Zn/Sr = 1; (c) EDX spectrum of the soft phase of (b); (d) EDX spectrum of the hard phase of (b); (e) Zn/Sr = 2; (f) Zn/Sr = 3; (g) $ZnFe_2O_4$.

temperatures is shown in Table I. Because the critical dimension of the soft phase has not reached the critical size at 900°C, the coercivity is the same as for the hard phase.[21] This implies that to reach the critical dimensions of the soft phase in the nano-structure composite, the particles must be heated at 1000°C.

Differential thermal analysis (DTA) and thermo-gravimetric (TGA) traces obtained from samples heated at 10°/min are shown in Fig. 5. In the DTA trace, the four peaks observed indicate that the nano-structure composite particles are formed by endothermic and exothermic reactions. The first endothermic peak at approximately 50°C is attributed to loss of water from the sample during heat treatment. The second endothermic peak at 695°C could arise because of conversion of hydroxide to oxides. The third exothermic peak at 805°C is attributed to the synthesis of such phases as Fe_2O_3, $ZnFe_2O_4$, and $SrFe_{12}O_{19}$. This is confirmed by the XRD analysis of the powder heat treated at 800°C. The fourth exothermic peak at 1040°C can be attributed to an exothermic reaction, resulting in the exchange coupling between the $ZnFe_2O_4$ and $SrFe_{12}O_{19}$ phases. This is also confirmed by the hysteresis loops (Fig. 4, HT at 1000°C). Hence, HT must be performed at >1000°C to lead to exchange coupling. TGA analysis of the as-synthesized powder shows weight loss was 27% in the temperature range from 15°C to 1200°C. This may be because of degassing and loss of moisture during the heat-treatment process.

As long as the length scale of the microstructure is smaller than the exchange length, magnetization anisotropy is reduced from its local value k_{loc} by exchange averaging over random local anisotropy[2]:

$$k_{\mathrm{loc}} = k\left(\frac{D}{l_{\mathrm{ex}}}\right)^{3/2} \tag{1}$$

The exchange length depends directly on the soft phase ratio.[2] The nucleation model predicts a modification of Brown's equation, known as the "modified Brown's equation", asserting that the coercivity field is given by[22]:

$$H_{\mathrm{c}} = 2\frac{k}{M_{\mathrm{s}}}\alpha_{\emptyset}\alpha_{\mathrm{ex}}\alpha_{k} - N_{\mathrm{z}}M_{\mathrm{s}} \tag{2}$$

where $\alpha_{\emptyset}$ is the orientation distribution of the grains in the magnet (in the randomly oriented structure

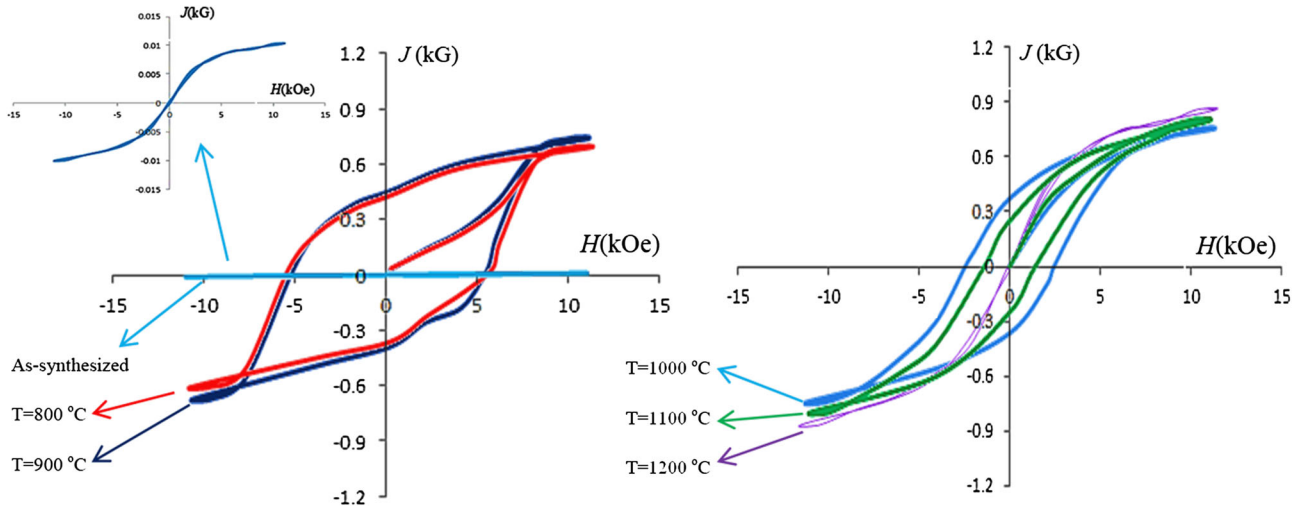

Fig. 5. Hysteresis loops of $SrFe_{12}O_{19}$–$ZnFe_2O_4$ nanostructure composite particles (Sr/Zn = 1), as-synthesized and after treatment at 800°C, 900°C, 1000°C, 1100°C, and 1200°C.

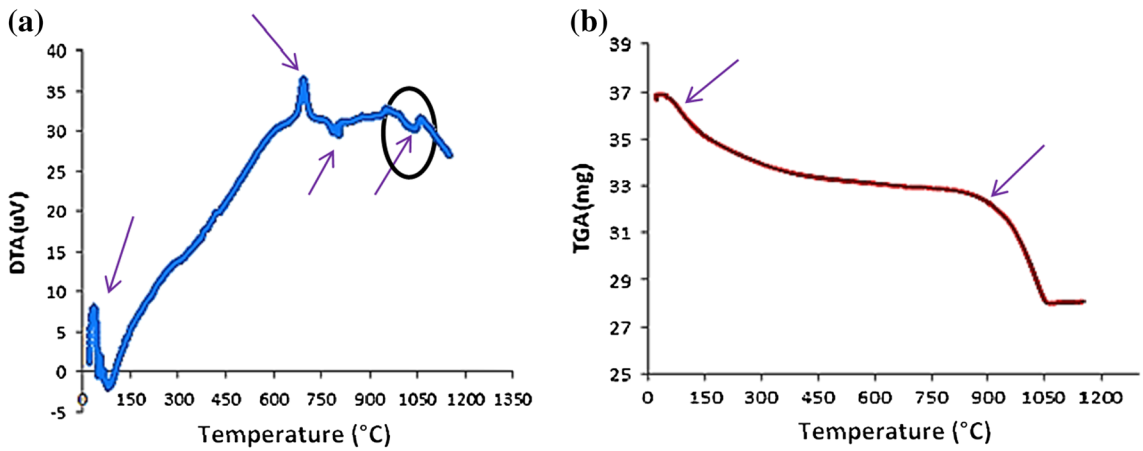

Fig. 6. (a) Differential thermal analysis (DTA) and (b) thermo-gravimetric analysis (TGA) traces, obtained at a heating rate of 10°/min, of the nano-structure composite particles.

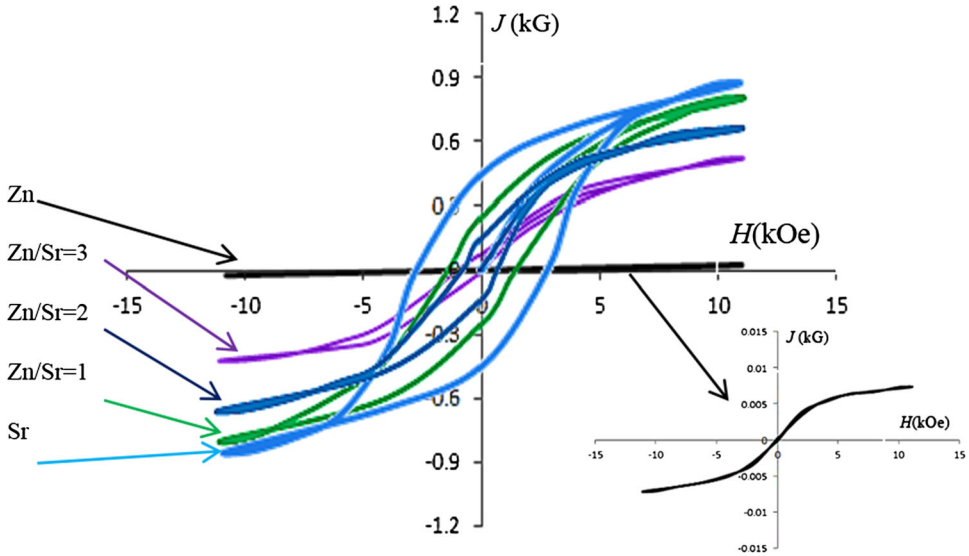

Fig. 7. Hysteresis loops of $SrFe_{12}O_{19}$–$ZnFe_2O_4$ nanostructure composite particles of different stoichiometry (Zn, Zn/Sr = 3, Zn/Sr = 2, Zn/Sr = 1, and Sr) heat treated at 1100°C.

Table III. Changing magnetic properties with Zn/Sr ratio

	Sr	Zn/Sr = 1	Zn/Sr = 2	Zn/Sr = 3	Zn
H_c(kOe)	2.410	1.493	0.757	0.175	0.027
J_s(kG)	0.80	0.70	0.59	0.45	0.08
Error bar	44.58	42.86	45.82	45.32	43.39

this is equal to 0.5), and the coefficient α_k takes into account the reduction in anisotropy in the region near the internal surface as a result of grain boundaries and interphases. The third coefficient, α_{ex}, is used to describe the effect of exchange coupling between neighboring grains on the coercivity field of the magnet. The x-ray diffraction results show that on increasing the temperature the amount of soft phase increases and the exchange length also increases. Therefore, α_{ex} and then H_c decrease.

The magnetic properties of nano-structure composite particles are shown for different Zn/Sr ratios in Fig. 6. Their saturation magnetization was found to depend on Zn/Sr ratio, decreasing from 0.80 kG to 0.08 kG as the Zn/Sr ratio was increased. This reduction in saturation magnetization with stoichiometric ratio (Zn/Sr) can be attributed to increased formation of the soft phase (zinc ferrite as antiferromagnetic material), as confirmed by the x-ray study of the powder heat treated at 1100°C (Fig. 1). In addition, the change in morphology may also affect the magnetic properties (Fig. 7).[4]

A coercivity of 1.4 kOe was observed for a Zn/Sr ratio of 1, decreasing thereafter to 0.15 kOe for a Zn/Sr ratio of 3. This decrease in coercivity with stoichiometric ratio can be attributed to an increase in the exchange-coupling interaction. The changing magnetic properties with Zn/Sr ratio are listed in Table III.

CONCLUSION

Uniform hexagonal plate and pyramid-shaped particles of the nanostructure composite $SrFe_{12}O_{19}$–$ZnFe_2O_4$ have been successfully synthesized by the co-precipitation method. The $SrFe_{12}O_{19}$–$ZnFe_2O_4$ nano-structure composite particles had higher saturation magnetization (0.85 kG) and lower intrinsic coercivity (0.09kOe) when heat treated at 1200°C, compared with the powder heat treated at 800°C (0.59 kG, 5.6 kOe), because of the exchange-coupling interaction between the hard and soft phases. The coercivity decreased and the saturation magnetization increased on increasing the treatment temperature. The coercivity also decreased, but the saturation magnetization was conditioned by increasing the Zn/Sr ratio.

OPEN ACCESS

REFERENCES

1. H. Zeng, J. Li, L. Wang, and S. Sun, *Lett. Nat.* 420, 395 (2002).
2. R. Handley, Modern magnetic materials Principle and Applications, A Wiley Interscience Publication, 2000.
3. Z. Liu, D. Zeng, R. Ramanujan, X. Zhong, and H.A. Davies, *J. Appl. Phys.* 105, 1 (2009).
4. H. Hsiang and R. Yao, *Mater. Chem. Phys.* 50, 1 (2007).
5. R. layer, R. Desia, and R. Upadhay, *J.Appl. Phys.* 47,180(2009).
6. S. Janasi, M. Emurea, F. Landgraf, and D. Rodrigues, *J. Magn. Magn. Mater.* 238, 168 (2002).
7. S. Saloomeh and A. Meibod, *P* (Waset: Pourafshary and H. Hosseini, 2010).
8. M. Bradiceanu, P. Vlazan, S. Novaconi, I. Grozescu, and P. Barvinchi, *Incemc.* 56, 19 (2007).
9. A. Texira, T. Ogasawara, and M. Nobrega, *Mat. Res.* 9, 257 (2006).
10. S. Tyagi, R. Agarwala, and V. Agarwala, *J. Mater. Sci.* 4, 125 (2009).
11. R. Mallik, *Nits*. 108, 40 (2012).
12. S. Tyagi, H. Baskey, R. Agawala, and T. Shami, *J. Electron. Mater.* 10, 11 (2011).
13. S. Tyagi, H. Baskey, R. Agarwala, V. Agrwala, and T. Shami, *Ceram. Int.* 37, 2631 (2011).
14. T. Gonzalez, A. Navarro, and C. Lopez, *J. Supercond. Nov. Magn.* 24, 549 (2011).
15. H. Wange, X. Xu, J. Zhang, and C. Li, *J. Mater. Sci.* 26, 1037 (2010).
16. T. Yang, H. Zhao, J. Han, N. Xu, Y. Shen, and J. Wang, *J. Eur. Cera. Soc.* 34, 1563 (2014).
17. F. Liu, F. Sommer, C. Bos, and E. Mittemijer, *Int. Mater. Rev.* 52, 193 (2007).
18. M. Rangolia, M. Chhanthbar, A. Tanna, K. Modi, G. Baldha, and H. Josi, *J. App. Phys.* 46, 66 (2008).
19. Z. Jin, C. Rockett, J. Liu, K. Hokamoto, and N. Thadhani, *Jim.* 46, 4 (2005).
20. B.D. Cullity and C.D. Graham, *Introduction to Magnetic Materials*, 2nd ed. (New York: Wiley, 2009).
21. H. Zeng, Sh Sun, J. Li, Z. Wang, and J.P. Liu, *Appl. Phys. Lett.* 85, 3 (2004).
22. H. Bertorello, P. Bercoff, and M. Oliva, *J. Magn. Magn. Mater.* 269, 122 (2004).